JOURNAL OF
ECOLOGY AND ENVIRONMENT
http://www.jecoenv.org

Research Paper
J. Ecol. Environ. 38(4): 461-476, 2015

Soil development and bacterial community shifts along the chronosequence of the Midtre Lovénbreen glacier foreland in Svalbard

Hye Young Kwon[1,†], Ji Young Jung[1,†], Ok-Sun Kim[2], Dominique Laffly[3], Hyoun Soo Lim[4] and Yoo Kyung Lee[1,*]

[1]Arctic Research Center, Korea Polar Research Institute, KIOST, Incheon 21990, Korea
[2]Division of Life Sciences, Korea Polar Research Institute, KIOST, Incheon 21990, Korea
[3]Department of Geography, University of Toulouse 2, Toulouse 31 058, France
[4]Department of Geological Sciences, College of Natural Science, Pusan National University, Busan 46241, Korea

Abstract

Global warming has accelerated glacial retreat in the high Arctic. The exposed glacier foreland is an ideal place to study chronosequential changes in ecosystems. Although vegetation succession in the glacier forelands has been studied intensively, little is known about the microbial community structure in these environments. Therefore, this study focused on how glacial retreat influences the bacterial community structure and its relationship with soil properties. This study was conducted in the foreland of the Midtre Lovénbreen glacier in Svalbard (78.9°N). Seven soil samples of different ages were collected and analyzed for moisture content, pH, soil organic carbon and total nitrogen contents, and soil organic matter fractionation. In addition, the structure of the bacterial community was determined via pyrosequencing analysis of 16S rRNA genes. The physical and chemical properties of soil varied significantly along the distance from the glacier; with increasing distance, more amounts of clay and soil organic carbon contents were observed. In addition, Cyanobacteria, Firmicutes, and Actinobacteria were dominant in soil samples taken close to the glacier, whereas Acidobacteria were abundant further away from the glacier. Diversity indices indicated that the bacterial community changed from homogeneous to heterogeneous structure along the glacier chronosequence/distance from the glacier. Although the bacterial community structure differed on basis of the presence or absence of plants, the soil properties varied depending on soil age. These findings suggest that bacterial succession occurs over time in glacier forelands but on a timescale that is different from that of soil development.

Key words: bacterial succession, chronosequence, glacier foreland, high arctic, soil development

INTRODUCTION

It is expected that climate change in the Arctic region would be much greater than the other regions (IPCC 2013). Climate change influences glacial ecosystems by affecting the advance and retreat of glaciers. Since the end of the Little Ice Age (LIA), glaciers have extensively retreated, and glacier foreland area has extended in the circumpolar region (Serreze et al. 2000). Glacier forelands provide great opportunities to study chronosequential changes through space-for-time substitutions; since the distance from the glacier terminus is a proxy for soil age,

http://dx.doi.org/10.5141/ecoenv.2015.049

Received 9 June 2015, **Accepted** 17 August 2015

***Corresponding Author**
E-mail: yklee@kopri.re.kr
Tel: +82-32-760-5530
[†]These authors contributed equally to this work. They should be considered as co-first authors.

pISSN: 2287-8327 eISSN: 2288-1220

the area close to the glacier edge is regarded as young soil and vice versa (Huggett 1998, Walker et al. 2010). Numerous studies have focused on soil development and primary succession of vegetation and microbes in glacier forelands (Matthews 1992, Wu et al. 2012, Zumsteg et al. 2012). However, most of the studies on proglacial succession have been conducted in subarctic and mountainous regions (Matthews 1992, Schmidt et al. 2008, Bernasconi et al. 2011, Wu et al. 2012). It has been proposed that the succession processes in the high Arctic may differ from those of other areas due to conditions such as low temperature, limited water and nutrient availability as well as the short growing season (Hodkinson et al. 2003).

Midtre Lovénbreen is one of the high Arctic glaciers, where several studies on primary succession of plants have been conducted in the glacier foreland. Plant communities in this area have been mapped using field surveys and scanned infrared aerial photography (Nilsen et al. 1999a, 1999b). In addition, Moreau et al. (2005) produced a detailed vegetation map showing that the stages of deglaciation and local conditions such as microtopography, microclimate, and runoff dynamics were important parameters for vegetation development.

Hodkinson et al. (2003) studied vegetation and soil development in the Midtre Lovénbreen foreland. They observed that the soil was colonized initially by cyanobacteria, one of the major components of ground cover for the first 60 years after glacial retreat, and vegetation cover increased gradually. Hodkinson et al. (2003) also showed organic matter accumulation along the chronosequence in the Midtre Lovénbreen foreland. They concluded that trends of vegetation and soil development in the high Artic generally corresponded to those in other ecosystems but on a longer timescale. White et al. (2007) used pyrolysis–gas chromatography–mass spectrometry to characterize soil organic carbon (SOC) in the same sampling site as that used by Hodkinson et al. (2003). They showed that SOC shifted from carbon signals derived from algae and animal to those from ligninaceous plants after 60–100 years of deglaciation.

Schütte et al. (2009, 2010) conducted studies regarding the structure of microorganisms in the Midtre Lovénbreen foreland. Schütte et al. (2009) collected soil samples from the same sampling site used by Hodkinson et al. (2003) to study soil bacterial succession using Terminal Restriction Fragment Length Polymorphism (T-RFLP). Although it was difficult to determine a linear and predictable pattern of succession at the time of the study, they found that bacterial communities were distinctly grouped according to soil age. When they later reanalyzed the same soil samples using 454-pyrosequencing, they concluded that bacterial phylotype richness and evenness increased as soil age increased, and that the turnover rate of the bacterial species was high in the initial phase of succession, the period between 5 to 19 years following deglaciation (Schütte et al. 2010).

Although various aspects of the Midtre Lovénbreen foreland have been studied, detailed information on the microbial community structure is still limited in this area. Moreover, the SOC fractionation which is to separate SOC depending on its lability and turnover time is one of the good approaches to study the sources and dynamics of SOC (Wander 2004). However, details on SOC characterization in the glacier foreland have not been studied very well. Furthermore, the relationship between soil development and microbial succession has not been studied in the Midtre Lovénbreen foreland. Therefore, we investigated the bacterial community structure via pyrosequencing, and measured several soil parameters to determine their patterns of change and to elucidate their relationships with bacterial community structure in the Midtre Lovénbreen foreland.

MATERIALS AND METHODS

Study site and soil sampling

The study area is located in the glacier foreland of Midtre Lovénbreen, Svalbard (78.9°N, 12.0°E). A line transect method was implemented to acquire soil samples from the glacial foreland in 2011. We sampled soil in the area from the glacier front to the outer LIA glacial maximum at a depth of 0–5 cm from seven sites where plant species or coverage had distinctly changed (ML1–7; Fig.1 and Table 1). All sampling sites were flat. The sites were categorized into the following four groups: average age since glacial retreat of 10.5 years, 33 years, 66 years, and outside the glacier moraine (Table 1). Three soil samples were collected from each site. For each sample, approximately 0.3 g of fresh soil was placed in RNAlater solution (Life technologies, Carlsbad, CA, USA) within 24 h of sampling and stored at 4°C for DNA extraction.

Physical and chemical analyses of soil

Gravimetric soil moisture content was determined by dividing the difference between fresh and dry soil weight by dry soil weight (24 h at 105°C).

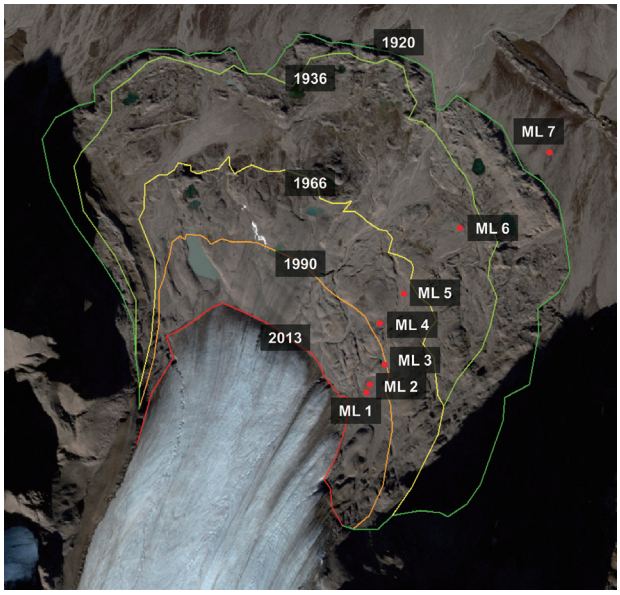

Fig. 1. A map of soil sampling sites and glacier retreat lines in the glacier foreland of Midtre Lovébreen.

$$\text{Soil moisture content (\%)} = \frac{\text{fresh soil weight} - \text{dry soil weight}}{\text{dry soil weight}} \times 100$$

The rest of the soil samples were dried at 45°C and passed through a 2-mm sieve to analyze their physical and chemical properties. Soil pH was measured with a pH meter (Orion TM Star A215; Thermo Fisher Scientific, Waltham, MA, USA) after mixing soil with deionized water (soil:water = 1:2 [w/v]) (Thomas 1996), and soil electrical conductivity (Orion TM Star A215; Thermo Fisher Scientific) was measured from the soil extract obtained by filtration of the soil suspension (soil:water = 1:5 [w/v]). Soil samples were ground to fine powder with a ball mill and sieved through a 250-μm sieve prior to analyzing total carbon (TC) and nitrogen (TN). The TC and TN contents in the soil samples were measured by the combustion method (950°C) using an elemental analyzer (FlashEA 1112; Thermo Fisher Scientific). The total inorganic carbon (TIC) content was determined by measuring the amount of CO_2 produced upon reaction of powdered soil samples with 42.5% phosphoric acid at 80°C using a CO_2 coulometer (CM5014; UIC Inc, Joliet, IL, USA). SOC content was calculated by determining the difference between the TC and TIC contents. Soil texture was analyzed after treating the soil samples with concentrated H_2O_2 (34.5%). The percentage of sand particles was determined by wet-sieving, and the percentages of silt and clay particles were determined using a Micrometrics Sedigraph 5120 (Micromeritics, Norcross, GA, USA). Density-size fractionation of SOC was completed using sodium polytungstate solution and wet-sieving as follows. 10 g of soil was mixed with 30 mL of a sodium polytungstate solution (density 1.55 g/cm^3), and the floating materials (light fraction [LF]) were collected by filtration through pre-combusted GF/A filters (Paré and Bedard-Haughn 2011). The remaining heavy fraction (HF) was mixed with a 0.5% sodium hexametaphosphate solution, dispersed via 18 h of shaking, and passed through a 53-μm sieve. The physical fractionation scheme, which was modified by Six et al. 2002, was as follows: materials larger than 53 μm comprised the sand plus intra-aggregate particulate organic matter (sand + iPOM) fraction, and those smaller than 53 μm comprised the mineral-associated SOC (mSOC) fraction. All fractions were dried at 45°C and weighed. The amount of sodium

Table 1. Vegetation cover and the glacier retreat period for sampling sites

Sampling site	GPS coordinates	Vegetation cover	Coverage (%)	Substrate	Glacier retreat period	Average age (years)
ML1	78°53′37.68″N 12°4′42.74″E	Bare soil	-	Sand	Between 2011-1990	10.5
ML2	78°53′38.80″N 12°4′44.71″E	Green algae and cyanobacteria	40	Gravel, sand		
ML3	78°53′41.29″N 12°4′53.82″E	Biological soil crust	5	Gravel, sand		
ML4	78°53′46.49″N 12°4′49.34″E	Sparse distribution of *Saxifraga oppositifolia*	10	Sand	Between 1990-1966	33
ML5	78°53′50.38″N 12°5′3.89″E	Bare soil	-	Gravel, sand		
ML6	78°53′59.02″N 12°5′38.28″E	*Salix polaris*	20	Gravel, sand	Between 1966-1936	66
ML7	78°54′9.03″N 12°6′34.47″E	*Salix polaris* and *Silene acaulis*	40	Sand, silt	Before LIA	No data

LIA, the Little Ice Age.

hexametaphosphate contained in the mSOC fraction was corrected. The sand + iPOM and mSOC fractions were acid-washed with 1 M HCl to remove TIC and then ground to a fine powder to analyze TC and TN. To determine the characteristics of SOC, ^{13}C nuclear magnetic resonance spectroscopy (NMR) analysis was performed on four samples in total: the LFs from ML4, ML6, and ML7 and the mSOC fraction from ML7. It was difficult to conduct ^{13}C NMR analysis for the other samples because they contained low concentrations of C. ^{13}C cross polarization/magic angle spinning NMR spectra were acquired on a 400 MHz Avance II+ Bruker Solid-state NMR spectrometer (Bruker Corporation, Billerica, MA, USA) at the Korea Basic Science Institute, Daegu, Korea. NMR peak areas were divided into four regions according to the following chemical shift limits: 0–45 parts per million (ppm; alkyl-C), 45–110 ppm (*O*/*N*-alkyl C), 110–160 ppm (aromatic C), and 160–220 ppm (carboxyl C) (Baldock et al. 1992, Kögel-Knabner et al. 1992).

DNA extraction

For each soil sample, total genomic DNA was extracted from 0.3 g of soil using commercially available DNA extraction kits (FDS-FastDNA® SPIN Kit for Soil; MP Biomedicals, Santa Anna, CA, USA) (Vishnivetskaya et al. 2014). All DNA extracts were stored at -20°C.

Amplification and 454 pyrosequencing

The hypervariable V1–V3 region (484 bp) of bacterial 16S rRNA was amplified from genomic DNA using the conserved primers 27f (5′-AGAGTTTGATCMTGGCTCAG-3′) and 519r (5′-GWATTACCGCGGCKGCTG-3′), which included a unique sequence tag to barcode each of the samples (Kim et al. 2011a). The 16S rRNA gene was amplified using a Thermocycler (Whatman Biometra 96-well PCR system; Biometra, Göttingen, Germany) with the following program conditions: 30 s at 94°C, 30 s at 55°C, and 1 min at 72°C for 25 cycles, followed by a final extension at 72°C for 10 min and subsequent cooling to 4°C. To ascertain the specificity of the PCR amplification, a negative control (PCR mix without DNA template) was included. The sizes of the PCR products were confirmed by electrophoresis on 1% agarose gels. The concentrations of the amplicons were estimated using a NanoDrop ND-1000 Spectrophotometer (NanoDrop Technologies Inc., Wilmington, DE, USA). Amplicons were purified using a PCR product purification kit (Labopass™ Gel; Cosmo Genetech, South Korea), and equal amounts of all amplicons were mixed in a single tube. DNA samples were sequenced using a GS FLX Titanium System (454 Life Sciences, Roche Applied Science, Penzberg, Germany). The amount and purity of extracted genomic DNA for samples from sites ML1, ML2, and ML5 were low, thus PCR amplification was not successful. Therefore, the samples from ML3, ML4, ML6, and ML7 were used for the subsequent steps.

Quality control, phylogenetic assignment, alignment, and clustering of sequences

An average of 7,000 sequences was obtained from each sample by 454-pyrosequencing. The sequences, which were contained in three standard flowgram format files (Schloss et al. 2009), were sorted into groups by sequence identifiers. The sequences from the raw data were trimmed to a targeted fragment using PyroTrimmer (Oh et al. 2012) and aligned using CLUSTOM (Hwang et al. 2013) at a threshold of 97% sequence similarity. Potential chimeras were identified using UCHIME and removed prior to further analysis. Each sequence was then assigned a phylogenetically consistent taxonomy based on its most closely related sequence. The assignment of sequences to operational taxonomic units (OTUs) was carried out using data from EzTaxon-e (Kim et al. 2011b). Sequence taxonomy assignments were made using RDP classifier (Release 10.4), with a threshold of 80%. The 51 most dominant *Acidobacteria* sequences were divided into 3 groups (Group 4, 6, 7). The sequences were further divided into 26 subgroups (Hugenholtz et al. 1998).

Statistical analysis

Prior to statistical analysis, the normality of data and constant variance of errors were examined. Data for soil physical and chemical properties were analyzed by one-way ANOVA (variable: site; R Development Core Team 2011). When significant differences were observed ($P < 0.05$), Tukey's test was used to separate the mean differences as a post-hoc analysis. All physical and chemical properties of soil were used for principal component analysis (PCA) to observe site characteristics.

To investigate changes in phylotype diversity, the richness estimators Chao1 and ACE and the Simpson and Shannon diversity indices were calculated using MOTHUR (Bunge and Barger 2008). Bacterial community composition along the chronosequence was calculated statistically with PRIMER6 (Primer-E Ltd, United Kingdom) using Bray–Curtis similarity.

RESULTS

Vegetation distribution

Vegetation distribution along the chronosequence in the Midtre Lovénbreen glacier foreland showed a sequential change in the species composition (Table 1). The number and cover of plant species increased with increasing soil age except at ML5. ML1 and ML5 contained bare soil, and 40% of soil surface was covered with green algae and cyanobacteria in ML2. The surface of ML3 was partially covered (5%) with biological soil crust. *Saxifraga oppositifolia* was first observed, and its coverage was 10% in ML4. The coverage of *Salix polaris* was 20% in ML6. Diverse vascular plants such as *S. polaris* and *Silene acaulis* covered 40% of ground in ML7, which was located outside the glacier moraine.

Physical and chemical properties of soil

The physical and chemical properties of soil samples taken from ML1–ML5 were generally different from those taken from the older sites, ML6 and ML7. The soil moisture content was as high as 15–30% in the samples from ML1, ML2, and ML3 but low in other sites (Table 2). Soil pH was mostly greater than 8.0 in the area close to the glacier but significantly lower in ML6 and ML7 (Table 2). Soil EC in ML1, ML2, ML3, and ML5 was significantly higher than that observed at the other sites (Table 2). Across all the sites, sand particles were predominant, and clay was the least abundant (Table 3). There were no significant differences among the sites in terms of the percentage of sand and silt particles, but the clay content in ML6 and ML7 was significantly higher than at the other five sites (Table 3). Soil from ML1 to ML5 was classified as sandy loam, and soil from ML6 and ML7 was classified as loam. There were trends indicating an increase in TC, SOC, and TN concentrations with increasing distance from the glacier, but the differences were not statistically significant among ML1-ML5 (Table 4). The SOC concentration was the highest in ML7 (2.8%), followed by that in ML6. The TIC and $CaCO_3$ concentrations were significantly higher

Table 2. Soil moisture content, pH, and electrical conductivity in each site

	ML1	ML2	ML3	ML4	ML5	ML6	ML7
MC (%)							
Mean	17.22^{c}	33.55^{a}	25.33^{b}	4.01^{de}	0.26^{e}	8.29^{d}	3.35^{de}
SD	(3.57)	(3.93)	(1.51)	(1.50)	(0.06)	(1.15)	(0.51)
Soil pH							
Mean	8.41^{ab}	8.40^{ab}	8.24^{bc}	8.35^{b}	8.65^{a}	8.05^{c}	7.64^{d}
SD	(0.10)	(0.02)	(0.04)	(0.07)	(0.09)	(0.11)	(0.16)
EC (mS cm^{-1})							
Mean	0.06^{a}	0.07^{a}	0.06^{a}	0.03^{b}	0.02^{b}	0.05^{a}	0.03^{b}
SD	(0.02)	(0.01)	(0.01)	(0.01)	(0.00)	(0.01)	(0.01)

MC, soil moisture content; EC, electrical conductivity.
Different lower case letters among sites indicate significant differences at $P < 0.05$.

Table 3. Soil texture for sampling sites

	ML1	ML2	ML3	ML4	ML5	ML6	ML7
Sand (%)							
Mean	72.30	54.08	82.35	57.23	71.91	50.35	47.64 ^{ns}
SD	(8.75)	(4.30)	(3.64)	(27.25)	(28.97)	(0.37)	(3.69)
Silt (%)							
Mean	19.28	36.90	13.20	36.09	23.71	32.08	36.28 ^{ns}
SD	(8.41)	(3.63)	(4.15)	(26.01)	(28.55)	(1.28)	(1.21)
Clay (%)							
Mean	8.42 ^{b}	8.99 ^{b}	4.45 ^{b}	6.64 ^{b}	4.33 ^{b}	17.49 ^{a}	16.05 ^{a}
SD	(2.31)	(0.84)	(1.60)	(1.46)	(1.83)	(1.49)	(3.37)
Soil texture	Sandy loam	Sandy loam	Loamy sand	Sandy loam	Sandy loam	Loam	Loam

ns, not significantly different.
Different lower case letters among sites indicate significant differences at $P < 0.05$.

at the sites affected by the glacier (ML1–ML6) than in ML7. The carbon-to-nitrogen (C/N) ratio tended to increase with the soil age and was the highest in samples from ML4 and ML6. The C/N ratio at ML1 was 7.1, which was significantly lower than that at ML7.

Density fractionation showed that all the samples contained very small quantities of the light fraction (LF). Like the concentration of SOC, the amount of LF increased along the chronosequence with increasing distance from the glacier: the LF ratio was about 0.3% in ML1–ML5 but rose to 2–3% in ML6 and ML7 (Table 5). In case of the heavy fraction (HF), weight-based percentage of the sand + iPOM fraction was significantly lower and the mSOC fraction was significantly higher for ML6 and ML7 than other sites. The SOC concentrations in the LFs showed an increasing trend with soil age, while the TN concentrations and C/N ratios in the LFs were not statistically different among sites (Table 6). The SOC and TN concentrations in the sand + iPOM and mSOC fractions were not different among ML1–ML5, but ML6 and ML7 had significantly higher SOC and TN concentrations than the other sites.

^{13}C NMR spectroscopy did not reveal large differences among the LFs from ML4, ML6, and ML7 (Fig. S1 a-c). On the other hand, chemical compositions of the mSOC fraction were greatly different from those of the LFs (Fig. S1 c, d). The *O*/*N*-alkyl ratio (45–110 ppm range) was more than 50% in the LFs, compared to the mSOC fraction

Table 4. Total carbon, soil organic carbon, total inorganic carbon, total nitrogen concentrations, and carbon-to-nitrogen ratio in sampling sites

	ML1	ML2	ML3	ML4	ML5	ML6	ML7
Total carbon (%)							
Mean	0.29^{c}	0.35^{c}	0.35^{c}	0.60^{c}	0.34^{c}	1.81^{b}	2.81^{a}
SD	(0.01)	(0.05)	(0.02)	(0.25)	(0.03)	(0.41)	(0.58)
Soil organic carbon (%)							
Mean	0.13^{c}	0.21^{c}	0.15^{c}	0.44^{c}	0.11^{c}	1.59^{b}	2.80^{a}
SD	(0.00)	(0.05)	(0.02)	(0.33)	(0.01)	(0.44)	(0.58)
Total inorganic carbon (%)							
Mean	0.16^{a}	0.15^{a}	0.21^{a}	0.15^{a}	0.23^{a}	0.22^{a}	0.01^{b}
SD	(0.00)	(0.01)	(0.02)	(0.08)	(0.02)	(0.04)	(0.00)
Calcium carbonate (%)							
Mean	1.31^{a}	1.22^{a}	1.72^{a}	1.27^{a}	1.93^{a}	1.81^{a}	0.10^{b}
SD	(0.03)	(0.06)	(0.13)	(0.63)	(0.19)	(0.33)	(0.01)
Total Nitrogen (%)							
Mean	0.019^{c}	0.019^{c}	0.015^{c}	0.026^{c}	0.009^{c}	0.092^{b}	0.185^{a}
SD	(0.003)	(0.000)	(0.001)	(0.015)	(0.002)	(0.027)	(0.036)
C/N ratio							
Mean	7.10^{c}	10.94^{bc}	10.11^{bc}	16.26^{a}	12.57^{ab}	17.39^{a}	15.12^{ab}
SD	(0.80)	(2.91)	(0.63)	(2.39)	(2.67)	(0.77)	(0.60)

Different lower case letters among sites indicate significant differences at $P < 0.05$.
C/N ratio, carbon-to-nitrogen ratio.

Table 5. Relative mass ratio of light fraction, sand plus intra-aggregate particular matter fraction, and mineral-associated soil organic carbon fraction after density-size fractionation

	ML1	ML2	ML3	ML4	ML5	ML6	ML7
Percentage of LF							
Mean	0.31^{c}	0.41^{c}	0.27^{c}	0.31^{c}	0.30^{c}	1.99^{b}	3.24^{a}
SD	(0.20)	(0.14)	(0.12)	(0.17)	(0.10)	(0.52)	(0.63)
Percentage of sand + iPOM fraction (greater than 53 μm)							
Mean	90.91^{a}	79.01^{ab}	92.97^{a}	69.29^{b}	96.04^{a}	61.07^{b}	65.80^{b}
SD	(6.94)	(5.04)	(2.82)	(14.86)	(1.77)	(2.88)	(1.35)
Percentage of mSOC fraction (less than 53 μm)							
Mean	8.78^{b}	20.58^{ab}	6.76^{b}	30.40^{a}	3.66^{b}	36.94^{a}	30.96^{a}
SD	(6.75)	(4.91)	(2.77)	(14.70)	(1.84)	(3.11)	(1.21)

LF, light fraction; sand+iPOC fraction, sand plus intra-aggregate particular matter fractions; mSOC fraction, mineral-associated soil organic carbon fraction.
Different lower case letters among sites indicate significant differences at $P < 0.05$.

which was approximately 30%. In the mSOC fraction, the proportion for aromatic C (110–160 ppm) and carboxyl C (160–210 ppm) was as high as 30% and 22%, respectively (Table 7).

PCA results showed that principal component (PC) 1 and PC 2 explained 54.2% and 15.0% of data variability, respectively. Thus, in total, 70% of variability was explained by two principal components. PC 1 was closely related to soil organic matter components, and PC 2 was related to the C/N ratio in each fraction, EC, and moisture content. Score plots showed that the three replicates from each site clustered (Fig. 2), showing that the variability within sites was less than variability among sites. ML3, ML4, and ML5 were located on the left side of PC1, whereas ML6 and ML7 were located on the right side of PC1.

Table 6. Carbon and nitrogen concentrations and carbon-to-nitrogen ratio in light fraction, sand plus intra-aggregate particular matter fraction, and mineral-associated soil organic carbon fraction after density-size fractionation of soil organic carbon

	ML1	ML2	ML3	ML4	ML5	ML6	ML7
Total carbon concentration in LF (%)							
Mean	7.92^{c}	15.61^{bc}	18.96^{abc}	22.67^{abc}	34.66^{a}	28.07^{ab}	31.30^{ab}
SD	(1.54)	(7.78)	(8.05)	(4.67)	(8.46)	(3.36)	(3.43)
Total Nitrogen concentration in LF (%)							
Mean	0.23	0.86	0.98	0.91	0.92	1.30	1.32^{ns}
SD	(0.10)	(0.41)	(0.75)	(0.12)	(0.64)	(0.07)	(0.11)
C/N ratio in LF							
Mean	37.49	18.15	29.17	25.58	45.14	21.50	23.68^{ns}
SD	(12.55)	(3.17)	(20.88)	(8.94)	(17.02)	(1.51)	(1.76)
Organic carbon concentration in sand+iPOC fraction (%)							
Mean	0.08^{c}	0.14^{c}	0.08^{c}	0.22^{c}	0.06^{c}	0.81^{b}	2.06^{a}
SD	(0.01)	(0.03)	(0.01)	(0.12)	(0.00)	(0.19)	(0.41)
Total nitrogen concentration in sand+iPOC fraction (%)							
Mean	0.004^{c}	0.007^{c}	0.004^{c}	0.017^{c}	0.007^{c}	0.041^{b}	0.123^{a}
SD	(0.001)	(0.002)	(0.001)	(0.010)	(0.001)	(0.011)	(0.025)
C/N ratio in sand+iPOC fraction (%)							
Mean	18.97^{a}	20.64^{a}	18.33^{a}	12.70^{bc}	9.54^{c}	20.11^{a}	16.74^{ab}
SD	(3.31)	(3.33)	(0.91)	(0.72)	(1.32)	(1.18)	(0.25)
Organic carbon concentration in mSOC fraction (%)							
Mean	0.22^{c}	0.21^{c}	0.29^{c}	0.18^{c}	0.35^{c}	0.84^{b}	1.36^{a}
SD	(0.05)	(0.07)	(0.04)	(0.02)	(0.08)	(0.12)	(0.09)
Total nitrogen concentration in mSOC fraction (%)							
Mean	0.013^{c}	0.012^{c}	0.022^{c}	0.013^{c}	0.028^{c}	0.064^{b}	0.128^{a}
SD	(0.003)	(0.003)	(0.004)	(0.002)	(0.006)	(0.012)	(0.005)
C/N ratio in mSOC fraction (%)							
Mean	16.85^{a}	16.74^{a}	13.07^{bc}	14.23^{ab}	12.32^{bc}	13.20^{bc}	10.68^{c}
SD	(2.13)	(1.15)	(1.49)	(0.60)	(0.04)	(0.59)	(0.45)

LF, light fraction, C/N ratio, carbon-to-nitrogen ratio; sand+iPOC fraction, sand plus intra-aggregate particular matter fractions; mSOC fraction, mineral-associated soil organic carbon fraction.
Different lower case letters among sites indicate significant differences at $P < 0.05$.
ns, not significantly different.

Table 7. Relative area ratio for major carbon functional groups in each soil organic carbon fraction acquired from nuclear magnetic resonance spectra

C functional groups / SOC fraction	Alkyl C (0-45 ppm)	O/N alkyl-C (45-110 ppm)	Aromatic C (110-160 ppm)	Carboxyl C (160-210 ppm)
ML4 Light fraction	22.1	51.0	15.0	11.9
ML6 Light fraction	22.5	52.1	12.5	12.9
ML7 Light fraction	25.6	48.8	11.9	13.6
ML7 mSOC fraction	22.3	29.6	29.6	21.5

SOC fraction, soil organic carbon fraction; mSOC fraction, mineral-associated soil organic carbon fraction.

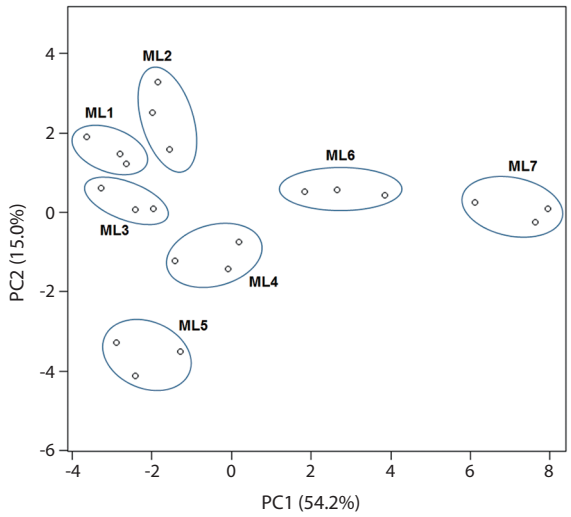

Fig. 2. Relative positions of sampling sites in the score plot of the principal component analysis (PCA). All measured physical and chemical properties of soil were used in PCA.

Bacterial diversity and community structure

Species diversity in soil samples was assessed by determining the number of OTUs with a threshold sequence similarity of 97%. Rarefaction curves from resampled sequences based on the lowest sequence readout (1,228 reads from the ML3 soil sample) revealed that bacterial diversity in all the sites increased with time (ML3 < ML4 < ML6 < ML7; Fig. S2).

The diversity indices at 97% sequence similarity, reflecting the overall soil bacterial community patterns along the glacier chronosequence, are shown in Table 8. When soil samples from ML3 and ML7 were compared, the difference in phylotype richness (i.e., number of OTUs) was approximately 323. Since the richness estimators Chao1 and ACE, and the Shannon diversity index are affected by the sequence read count, bacterial diversity was found to have increased over time (Table 8).

The relative abundance of bacterial communities at the phylum level showed a high proportion of Proteobacteria and Actinobacteria in all samples and the highest proportion of Cyanobacteria in the early stage of glacier recession (Fig. 3). The bacterial community in ML3 (20-years-old) soil was composed of Cyanobacteria (22.7%), Proteobacteria (22.0%), Actinobacteria (21.0%), Bacteroidetes (15.6%), and Firmicutes (9.4%). The relative abundance of Cyanobacteria was dramatically reduced in ML4. In ML4, Proteobacteria (25.2%), Actinobacteria

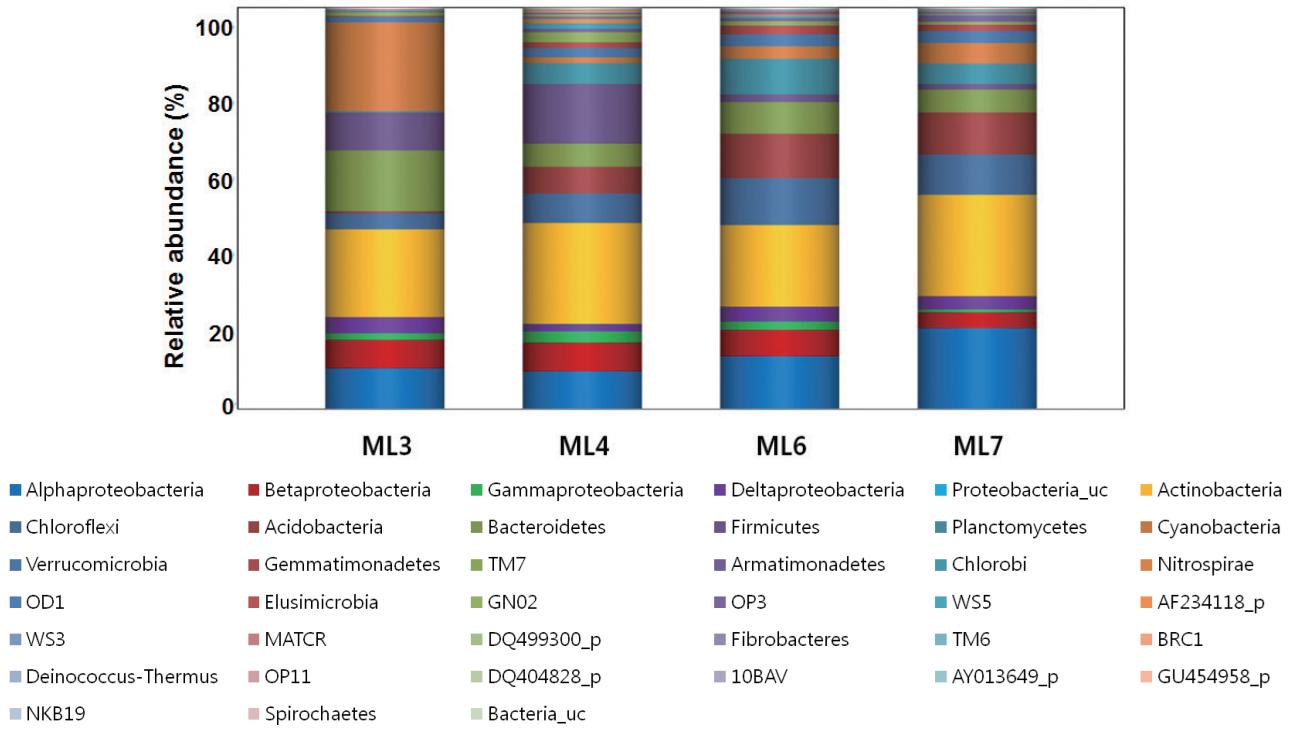

Fig. 3. Relative abundance of bacterial phyla along the chronosequence since glacier retreat.

ML3	ML4	ML6	ML7	OTUs	Phylum	Class	Order	Family	Genus	Species	Acc. No.	Identity %
9.8	37.6	4.8	2.7	OTU_1	Firmicutes	Bacilli	Bacillales	Bacillaceae	Bacillus_g26	*Bacillus pseudalcaliphilus*	X76449	92
5.8	11.6	5.5	0.4	OTU_2	Actinobacteria	Actinobacteria_c	Micrococcales	Intrasporangiaceae	Oryzihumus	*HQ462540_s*	HQ462540	97
22.3	6.9	1.2	0.0	OTU_3	Actinobacteria	Actinobacteria_c	Micrococcales	Intrasporangiaceae	Oryzihumus	*GQ397075_s*	GQ397075	96
0.0	0.3	11.3	10.6	OTU_4	Acidobacteria	Chloracidobacterium_c	Blastocatella_o	AY281358_f	AY281358_g	*FJ479144_s*	FJ479144	99
17.0	0.3	1.3	3.5	OTU_5	Cyanobacteria	Chroobacteria	Oscillatoriales	Pseudanabaenaceae	Pseudanabaena	*Pseudanabaena tremula*	AF218371	100
3.5	2.2	5.3	2.4	OTU_6	Proteobacteria	Alphaproteobacteria	Sphingomonadales	Sphingomonadaceae	Sphingomonas	*FM211709_s*	FM211709	99
0.2	2.4	2.4	3.8	OTU_7	Proteobacteria	Alphaproteobacteria	Rhizobiales	Rhodoligotrophos_f	AF370880_g	*FM877535_s*	FM877535	99
4.0	2.1	4.3	0.0	OTU_8	Actinobacteria	Actinobacteria_c	Micrococcales	Intrasporangiaceae	Oryzihumus	*HQ462540_s*	HQ462540	96
0.0	1.3	2.0	4.8	OTU_9	Actinobacteria	Thermoleophilia	Solirubrobacterales	EU861899_f	EU861899_g	*Patulibacter ginsengiterrae*	EU710748	96
0.2	3.8	1.9	0.2	OTU_10	Actinobacteria	Actinobacteria_c	Micrococcales	Dermatophilaceae	Austwickia	*Austwickia chelonae*	AJ243919	94
0.0	0.6	3.7	3.6	OTU_11	Actinobacteria	Actinobacteria_c	Frankiales	Nakamurellaceae	Nakamurella	*JF417732_s*	JF417732	97
0.0	0.2	9.5	0.0	OTU_12	Acidobacteria	HQ645210_c	HQ645210_o	HQ645210_f	HQ190481_g	*HQ190351_s*	HQ190351	97
12.7	0.0	0.0	0.0	OTU_13	Bacteroidetes	Bacteroidia	Bacteroidales	Paludibacter_f	Paludibacter_f_uc	*AJ488070_s*	AJ488070	94
0.9	1.1	4.5	1.5	OTU_14	Actinobacteria	Actinobacteria_c	Micrococcales	Intrasporangiaceae	Oryzihumus	*HQ462540_s*	HQ462540	97
0.0	0.6	1.9	4.3	OTU_15	Proteobacteria	Alphaproteobacteria	Rhodospirillales	Acetobacteraceae	EU861940_g	*AM696989_s*	AM696989	96
1.2	2.9	1.7	0.1	OTU_16	Actinobacteria	Actinobacteria_c	Micrococcales	Intrasporangiaceae	Oryzihumus	*GQ397075_s*	GQ397075	96
0.0	0.0	1.5	5.1	OTU_17	Proteobacteria	Alphaproteobacteria	Rhizobiales	Hyphomicrobiaceae	EU753663_g	*FJ455876_s*	FJ455876	94
0.9	0.3	0.9	4.3	OTU_18	Cyanobacteria	Chroobacteria	Oscillatoriales	Pseudanabaenaceae	DQ181682_g	*DQ181682_s*	DQ181682	99
0.0	0.0	0.9	5.3	OTU_19	Actinobacteria	Actinobacteria_c	Pseudonocardiales	Pseudonocardiaceae	Pseudonocardia	*Pseudonocardia mongoliensis*	AB521671	98
0.0	0.1	0.1	5.8	OTU_20	Proteobacteria	Alphaproteobacteria	Rhodospirillales	Acetobacteraceae	EU861940_g	*EU861940_s*	EU861940	95
0.0	0.2	0.5	5.1	OTU_21	Actinobacteria	Thermoleophilia	Solirubrobacterales	Solirubrobacteraceae	Solirubrobacter	*FJ479288_s*	FJ479288	97
0.0	2.8	1.2	0.4	OTU_22	Nitrospirae	Nitrospira_c	Nitrospirales	Nitrospiraceae	Nitrospira	*DQ058676_s*	DQ058676	99
0.0	0.4	4.3	1.6	OTU_23	Chloroflexi	Anaerolineae	Anaerolinaeles	Anaerolinaceae	GQ500701_g	*AB240474_s*	AB240474	99
0.2	0.2	2.7	2.5	OTU_24	Chloroflexi	Chloroflexi_c	Chloroflexales	FJ479330_f	FJ478841_g	*GQ397052_s*	GQ397052	96
0.2	1.8	1.2	1.1	OTU_25	Proteobacteria	Alphaproteobacteria	Rhizobiales	Rhodoligotrophos_f	AF370880_g	*GQ396960_s*	GQ396960	99
1.6	2.6	0.0	0.0	OTU_26	TM7	TM7_c	TM7_o	TM7_f	TM7_g	*AJ318136_s*	AJ318136	98
0.0	0.2	0.8	3.7	OTU_27	Proteobacteria	Alphaproteobacteria	Rhizobiales	Bradyrhizobiaceae	Bradyrhizobium	*Bradyrhizobium canariense*	AJ558025	100
0.5	1.7	1.5	0.4	OTU_29	Proteobacteria	Betaproteobacteria	AB308366_o	HQ014645_f	HQ014645_g	*EF516814_s*	EF516814	98
0.0	1.2	1.3	1.5	OTU_30	Acidobacteria	EU686603_c	EU686603_o	EU686603_f	EU861837_g	*EF688341_s*	EF688341	99
0.0	2.7	0.0	0.0	OTU_31	Acidobacteria	HQ645210_c	HQ645210_o	HQ645210_f	HQ190481_g	*AY921884_s*	AY921884	97
2.1	0.5	1.2	1.1	OTU_32	Proteobacteria	Alphaproteobacteria	Sphingomonadales	Sphingomonadaceae	Sandarakinorhabdus	*FR682701_s*	FR682701	100
0.7	2.4	0.1	0.0	OTU_33	Actinobacteria	Actinobacteria_c	Corynebacteriales	Nocardiaceae	Nocardia	*Nocardia nova*	Z36930	99
0.0	0.7	0.5	2.5	OTU_34	Chloroflexi	GQ396871_c	GQ396871_o	GQ396871_f	GQ396871_g	*GQ396871_s*	GQ396871	98
4.7	0.8	0.0	0.0	OTU_35	Proteobacteria	Betaproteobacteria	Burkholderiales	Comamonadaceae	Rhodoferax	*Rhodoferax fermentans*	D16211	99
0.5	0.5	3.5	0.3	OTU_36	Proteobacteria	Betaproteobacteria	Burkholderiales	Oxalobacteraceae	EU636042_g	*EU636042_s*	EU636042	98
0.0	0.0	0.0	3.6	OTU_37	Proteobacteria	Alphaproteobacteria	Rhodospirillales	Acetobacteraceae	EU861940_g	*AM696989_s*	AM696989	100
0.0	0.7	0.1	2.5	OTU_38	Actinobacteria	Actinobacteria_c	Kineosporiales	Kineosporiaceae	Kineosporia	*Kineosporia rhamnosa*	AB003935	98
0.0	0.0	0.0	3.6	OTU_39	Proteobacteria	Alphaproteobacteria	Rhodospirillales	Acetobacteraceae	EU861940_g	*AY192273_s*	AY192273	95
6.5	0.0	0.0	0.0	OTU_40	Cyanobacteria	Hormogoneae	Nostocales	Nostocaceae	Trichormus	*Trichormus variabilis*	DQ234832	97
0.0	1.3	0.4	1.3	OTU_41	Acidobacteria	Chloracidobacterium_c	Blastocatella_o	Blastocatella_f	Blastocatella	*AY395388_s*	AY395388	98
2.1	0.3	1.3	0.9	OTU_42	Firmicutes	Clostridia	Clostridiales	Clostridiaceae	Clostridium	*Clostridium estertheticum subsp. laramiense*	AJ506115	97
0.0	0.2	2.1	1.5	OTU_43	Gemmatimonadetes	Gemmatimonadetes_c	Gemmatimonadales	Gemmatimonadaceae	EU421850_g	*EU421850_s*	EU421850	97
0.0	0.1	1.5	2.2	OTU_44	Proteobacteria	Betaproteobacteria	Burkholderiales	Sphaerotilus_f	AM777983_g	*AJ964894_s*	AJ964894	96
0.4	1.2	1.3	0.3	OTU_45	Proteobacteria	Betaproteobacteria	Burkholderiales	Comamonadaceae	Polaromonas	*Polaromonas glacialis*	HM583568	99
0.0	0.8	1.3	1.0	OTU_46	Proteobacteria	Alphaproteobacteria	Rhizobiales	Bradyrhizobiaceae	DQ123621_g	*EU937939_s*	EU937939	98
0.4	0.2	0.3	2.4	OTU_47	Cyanobacteria	Gleobacteria	Gloeobacterales	Gloeobacteraceae	Gloeobacter	*Gloeobacter violaceus*	BA000045	95
0.2	1.4	1.3	0.0	OTU_48	Proteobacteria	Betaproteobacteria	EU786132_o	EU786132_f	EU786132_g	*AB252928_s*	AB252928	98
0.0	0.0	1.7	1.8	OTU_49	Cyanobacteria	Hormogoneae	Nostocales	Nostocaceae	Toxopsis	*AY493596_s*	AY493596	100
0.0	0.3	3.7	0.0	OTU_50	Proteobacteria	Betaproteobacteria	Burkholderiales	Comamonadaceae	Variovorax	*Variovorax ginsengisoli*	AB245358	99
1.4	0.8	1.2	0.3	OTU_51	Actinobacteria	Actinobacteria_c	Micrococcales	Intrasporangiaceae	Oryzihumus	*HQ462540_s*	HQ462540	96

Fig. 4. Heat map showing the 51 most dominant operational taxonomic units (OTUs).

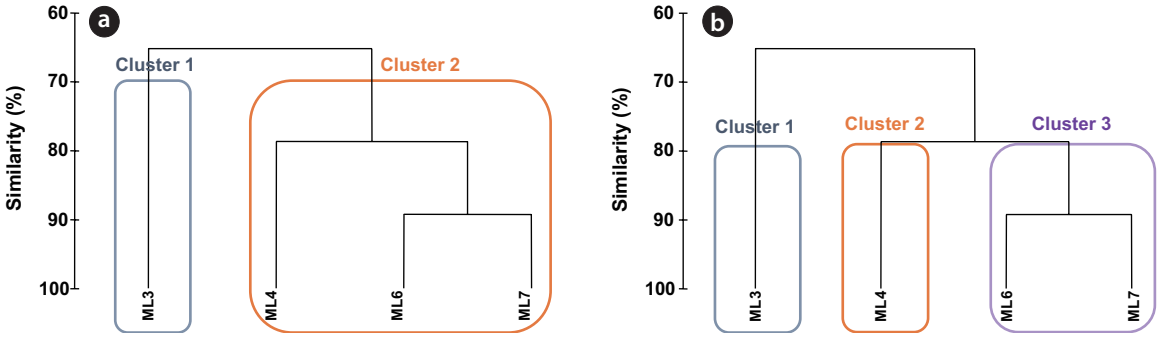

Fig. 5. Analysis of bacterial communities by clustering at the threshold of 70% (a) and 80% Bray–Curtis similarity (b).

(25.0%), Firmicutes (14.8%), and Chloroflexi (7.3%) were the most prevalent. In ML6, Proteobacteria (25%) and Actinobacteria (20%) were also present with Chloroflexi and Acidobacteria found in equal proportions (both 11%). In ML7, which was unaffected by the glacier, the bacterial community was composed of Proteobacteria (28%), Actinobacteria (25%), Acidobacteria (10%), and Chloroflexi (10%).

The subdivisions within the bacterial community were examined by performing a heat map analysis at the level of OTUs (Fig. 4). A representative 3% of the 2,116 OTUs were analyzed. In ML3, the abundant OTUs were OTU-3 (22.3%) and OTU-5 (17.0%). OTU-3 and OTU-5 showed the highest similarity with *Oryzihumus* species in Actinobacteria and *Pseudanabaena tremula* of the order Oscillatoriales in Cyanobacteria, respectively. OTU-40 (6.5%) was also abundant, which had 97% similarity with *Trichormus variabilis* of the order Nostocales in Cyanobacteria. In ML4, OTU-1 that showed 92% similarity with the sequence of *Bacillus pseudalcaliphilus* in Firmicutes was most frequently found (37.6%), and OTU-2 and OTU-3 belonging to Oryzihumus were also abundant. In ML6 and ML7, OTU-4 belonging to Acidobacteria was detected at a high rate (≥10%), which was derived from culture-independent, environmental clone library surveys. In addition, various other OTUs mostly belonging to the phyla Actinobacteria, Acidobacteria, and Alphaproteobacteria were observed in these two sites.

The bacterial community was classified into two clusters based on 70% Bray–Curtis similarity; cluster 1 included ML3, and cluster 2 included ML4, ML6, and ML7 (Fig. 5a). The two clusters of the bacterial community were divided depending on the abundance of Cyanobacteria (Fig. 5). On the other hand, bacterial community was grouped into three clusters based on the Bray–Curtis similarity index, using a threshold value of 80%: cluster 1 for ML3, cluster 2 for ML4, and cluster 3 for ML6 and ML7 (Fig. 5b). Cyanobacteria were highly represented in cluster 1; cluster 2 mainly consisted of Firmicutes; and cluster 3 had a high proportion of Chloroflexi and Acidobacteria.

Table 8. Phylotype diversity changes along the chronosequence

Sample	OTUs*	Diversity index			
		Chao	ACE	Shannon	Simpson
ML3	315	692.06	1107.41	4.58	0.03
ML4	529	1357.1	2488.53	5.42	0.02
ML6	634	1630.96	3364.71	6.03	0
ML7	638	1743.82	3145.94	6.05	0
Total	2116				

*OTUs defined as sequences with 97% similarity.

DISCUSSION

Vegetation succession in the glacier foreland

Vegetation distribution along the chronosequence in this study site generally followed the previously reported pattern of plant establishment in the Midtre Lovénbreen foreland (Nilsen et al. 1999b, Moreau et al. 2008). *S. oppositifolia* was first observed in ML4, where deglaciation had occurred between 1996 and 1999. *S. oppositifolia*, one of the pioneer species found after glacier retreat (Kume et al. 2003), had occurred all over the Midtre Lovénbreen foreland regardless of soil age (Moreau et al. 2008). *S. polaris* was found in ML6, where deglaciation had occurred between 1936 and 1966. *S. polaris* and *S. acaulis* were found in ML7. Moreau et al. (2008) had previously reported that the colonization of *S. polaris* and *S. acaulis* greatly increased after 70 and 100 years of deglaciation, respectively.

Soil development in the glacier foreland

Changes in soil properties in Midtre Lovénbreen foreland became obvious after 45-75 years since deglaciation. Several soil parameters related to soil development such as soil pH, clay and SOC contents, and amount of LF were significantly different between ML1-ML5 and ML6 sites (Tables 2–5). Moreover, soil pH, SOC and LF contents in ML6 were significantly different from those in ML7. These patterns were reflected in the distribution of study sites on the score plot by PCA (Fig. 2); ML1-ML5 were gathered on the left side of PC1, and ML6 and ML7 were distinctly grouped on the right side of PC2.

Soil pH decreased as soil age increased (Table 2). It is quite common to observe decreases in soil pH with soil age in glacier foreland chronosequences. Young soil contains a relatively low amount of organic matter and clay minerals, and thus base leaching could be enhanced under low cation exchange capacity (Matthews 1992).

While the percentages of sand and silt were not significantly different across all sites, ML6 showed significantly increased clay content (Table 3). Soil textural changes across the chronosequence in the glacial moraine are not always apparent (Jacobson and Birks 1980, Bernasconi et al. 2011) but can be relatively rapid when cryogenic and aeolian processes occur (Matthews 1992). The presence of vegetation cover can also influence soil texture by facilitating aeolian deposition (Matthews 1992). Consequently, the rate of change in soil properties following glacier retreat can vary widely depending on climate factors or other influences (Messer 1988).

Density–size fractionation of SOC showed that the proportion of LF in this study site was very low compared to the values reported from other high Arctic sites (Table 5); the LF was reported to be approximately 18% in Troulove, Canada (Paré and Bedard-Haughn 2011) and 7% in other sites in Svalbard (Jung et al. 2014). The low amount of LF might be attributed to low vegetation cover and the short period since deglaciation for vegetation establishment. The sand plus intra-aggregate particulate organic matter (sand + iPOM) fraction significantly increased in ML6 (Table 5). Since the sand + iPOM fraction included the particulate organic matter occurring within aggregates (Six et al. 2002), we could infer that the aggregation became an important mechanism for SOC protection after average 60 years of deglaciation. Although the mSOC fraction could contain relic organic carbon, assuming that all glacier-affected areas had started from the same initial conditions, the quantity from relic carbon would be less than 0.4%, which was the highest SOC content found in ML1–ML5 (Table 4). Therefore, the increase in the SOC content in the mSOC fraction from ML6 indicates the association of SOC with mineral particles and the humification processes that took place following deglaciation. The organo-mineral associations would have led to an increase in cation exchange capacity (Matthews 1992), and the associated SOC would have different chemical characteristics depending on the major carbon sources present during the initial soil formation (Dümig et al. 2012).

^{13}C NMR spectroscopy of the LF in ML4, ML6, and ML7 showed that the quality of organic matter did not differ by plant species (Table 7). As vascular plants were growing in ML4, ML6, and ML7, plant litter would have been a main component of the LFs in these sites. On the other hand, when comparing ^{13}C NMR spectroscopy between the LF and mSOC fraction for the site ML7, the proportion of the *O*/*N*-alkyl groups was less in the mSOC fraction than LF despite the similar proportion of alkyl-C groups between two fractions. While the *O*/*N*-alkyl group is a labile form of carbon and characteristic of carbohydrates, the alkyl-C is associated with recalcitrant waxy compounds and microbial-derived lipids (Baldock et al. 1992, Kögel-Knabner et al. 1992, Sohi et al. 2005, Marín-Spiotta et al. 2008). Marín-Spiotta et al. (2008) reported that the proportion of *O*-alkyl groups decreased and the proportion of alkyl-C groups increased as plant materials were transformed to SOC through decomposition. Therefore, the higher *O*/*N*-alkyl ratio in the LF than the mSOC fraction well represented the labile characteristics of LF.

Change in bacterial diversity and community structure along the glacier chronosequence

Bacterial diversity was found to have increased over time (Table 8). This result corresponds to a general change in bacterial diversity as soil developed in the glacier foreland, as has been observed in previous studies (Nemergut et al. 2007, Schütte et al. 2009, Jangid et al. 2013). Simpson's index ranges from zero for heterogeneity to one for homogeneity (Wu et al. 2012). Simpson's index for ML6 and ML7 was zero, but for the other two sites, it was greater than zero (Table 8). Therefore, all diversity indices indicated that the diversity of the bacterial community in the glacier foreland increased and that the characteristics of the foreland ecosystems changed from homogeneous to heterogeneous as succession proceeded (Schütte et al. 2009, Wu et al. 2012).

Cyanobacteria were the predominant phylum in the early period following glacier recession (Fig. 3). Among Cyanobacteria, Nostocales and Oscillatoriales were domi-

nant in the ML3 site (Table 3). Turicchia et al. (2005) also found that *Nostoc* spp. were abundant after 5 years and 19 years of glacier recession in the Midtre Lovénbreen foreland. Cyanobacteria are autotrophic organisms that use light energy. Cyanobacteria can play a crucial role in ecosystem development, particularly in oligotrophic environment like glacial foreland, because they can fix carbon and nitrogen (Schmidt et al. 2008, Schulz et al. 2013). Carbon and nitrogen are necessary for the settlement of other heterotrophs and plants. Cyanobacteria can also stabilize soil through producing exopolysaccharides (Schmidt et al. 2008, Schulz et al. 2013). There are several reports on the dominance of Cyanobacteria in the early stage of primary succession as well as near glacier fronts in the Arctic (Turicchia et al. 2005, Brankatschk et al. 2011, Schulz et al. 2013). Thus, the fact that Cyanobacteria were found in the highest abundance in ML3 is consistent with other findings.

The abundance of *Bacillus* spp. was highest in ML4 and ML3 (37.6% and 9.8%, respectively) (Fig. 3). *Bacillus* can exist under extreme conditions as endospores (Reddy et al. 2008). Jangid et al. (2013) also reported that the phylotype of a Firmicutes-related gene was dominant in the early stages of glacier recession in the Franz Josef glacier foreland. Thus, our observation of the predominance of *Bacillus* in the early stages of succession was consistent with that from the previous study.

The soil characteristics and bacterial community structure had changed along the chronosequence; the abundance of Acidobacteria increased, the proportion of Actinobacteria decreased, and soil pH decreased (Fig. 3 and Table 2). There have been numerous studies showing that soil pH influences bacterial community composition (Fierer and Jackson 2005, Knelman et al. 2012). Lauber et al. (2009) demonstrated in a continental scale study that whereas Acidobacteria were abundant in soil with a low pH (4–6), Actinobacteria were abundant in soil with a high pH (6.7–8.9). Although the range of the soil pH was not wide in this study area, the abundance of Actinobacteria was higher in ML3, where the soil pH was 8.2, and Acidobacteria were more abundant in ML6 and ML7, where the soil pH was 7.5–8.1 (Fig. 3 and Table 2). In addition, we tried the RDP ver. 10.4 classifier to classify our Acidobacteria DNA sequences into Acidobacterial subgroups. Most of them were classified into subgroup 4, 6, and 7, which were more abundant in higher pH (pH 6.0–8.5) (Jones et al. 2009). Therefore, the dominance of Acidobacteria in the pH range of 7.5–8.2 of our study site was consistent with the results from Jones et al. (2009).

Differences between bacterial community succession and soil development

Our results showed a discrepancy between the changes in soil characteristics and bacterial succession along the chronosequence. The bacterial community of this area seemed to be influenced more by plants than by soil properties. The bacterial community was classified into two clusters based on 70% Bray–Curtis similarity depending on the presence of plants. While ML3 was the only component in cluster 1 with a high abundance of Cyanobacteria, cluster 2 was composed of ML4, ML6, and ML7 where vascular plants were established (Fig. 5a). In contrast, soil characteristics were not different between ML3 and ML4, but they were significantly different from soil properties in ML6 and ML7 (Tables 2–5). The presence of plants had a great influence on the microbial community structure (Miniaci et al. 2007, Walker et al. 2010, Philippot et al. 2011, Knelman et al. 2012), showing that the bacterial community would change via interactions with plant species as vegetation cover was established (Wallenstein et al. 2007). In case of soil, the quantity of root exudates or plant litter would be very small, and the decomposition rate would be faster in young soils (Esperschütz et al. 2011). Therefore, the contribution of plant material to SOC would be minor in the early stages of succession. The fact that soil development appears to require more time than bacterial community change could account for the observed discrepancy between soil properties and bacteria distribution.

In addition, although SOC contents between ML6 and ML7 were significantly different, there were no differences in bacterial community composition between the two sites despite a great age difference (Tables 1, 4). The bacterial community in ML6 and ML7 was grouped into the same cluster based on the Bray–Curtis similarity index, using a threshold value of 80% (Fig. 5b). In addition, diversity indices and the number of OTUs did not differ between ML6 and ML7 when phylotype richness (OTU) was compared at the threshold of 97% similarity (Table 8). In contrast, ML6 and ML7 were separated into two distinct groups when soil characteristics were analyzed by PCA (Fig. 2). Schütte et al. (2010) found that the turnover rate of the bacterial community in the Midtre Lovénbreen foreland was approximately 7% per year for the first 14 years following glacier retreat and then decreased to approximately 0.7% per year by 100 to 150 years. The study from Tianshan No. 1 glacier foreland in China also showed that the turnover rate tended to decrease over time. Jangid et al. (2013) suggested that bacterial community dy-

namics were well correlated with pedogenesis in the early stages of succession but remained constant regardless of soil development during the advanced stages of ecosystem development. Similarly, our results showed that the bacterial community composition remained stable in the later stages of succession. However, the reason for this phenomenon is still not clear.

CONCLUSION

In this study, we showed bacterial community structure and soil characteristics along the chronosequence of the Midtre Lovénbreen glacier foreland. Climate warming has accelerated the glacier retreat and exposed rapidly the hidden ground below the glacier. In this newly exposed land, the SOC accumulation would be initiated by the settlement of various bacterial groups before plant colonization. Moreover, the bacterial community seemed to be influenced by the presence of plants rather than soil development. Therefore, if the kinds and the colonization rate of plant species have been changed due to climate warming, the bacterial community succession would also be influenced.

In addition, the glacier foreland contained various microtopography and has been influenced by several disturbances. Therefore, plant colonization is not uniform and spatially very heterogeneous in the glacier foreland. The limited number of samples would not completely cover spatial variability and prevent an elucidation of general trends of changes in bacterial community and soil development. The heterogeneity of the study area should be considered for the interpretation of the results. However, this is a worthwhile preliminary study showing that the bacterial community composition and soil properties changed with soil age. We also showed that the patterns/time scale of bacterial succession and soil development were different. Accordingly, to elucidate further relationship between bacterial succession and soil development, it will be necessary to conduct additional studies using more samples.

ACKNOWLEDGMENTS

This study was supported by the National Research Foundation of Korea, which is funded by the Korean Government (MSIP) (NRF-2011-0021063, 0021067) (PN15082, KOPRI). This study was also supported by Korea Polar Research Institute (PE15030) and by the Korea Research Council of Fundamental Science & Technology (BSPG11040-252-7).

LITERATURE CITED

Baldock JA, Oades JA, Waters AG, Peng X, Vassallo AM, Wilson MA. 1992. Aspects of the chemical structure of soil organic materials as revealed by solid-state ^{13}C NMR spectroscopy. Biogeochemistry 16: 1-42.

Bernasconi SM, Bauder A, Bourdon B, Brunner I, Bünemann E, Chris I, Derungs N, Edwards P, Farinotti D, Frey B, Frossard E, Furrer G, Gierga M, Göransson H, Gülland K, Hagedorn F, Hajdas I, Hindshaw R, Ivy-Ochs S, Jansa J, Jonas T, Kiczka M, Kretzschmar R, Lemarchand E, Luster J, Magnusson J, Mitchell EAD, Venterink HO, Plötze M, Reynolds B, Smittenberg RH, Stähli M, Tamburini F, Tipper EF, Wacker L, Welc M, Wiederhold JG, Zeyer J, Zimmermann S, Zumsteg A. 2011. Chemical and biological gradients along the Damma glacier soil chronosequence, Switzerland. Vadose Zone J 10: 867-883.

Brankatschk R, Töwe S, Kleineidam K, Schloter M, Zeyer J. 2011. Abundances and potential activities of nitrogen cycling microbial communities along a chronosequence of a glacier forefield. ISME J 5: 1025-1037.

Bunge J, Barger K. 2008. Parametric models for estimating the number of classes. Biom J 50: 971-982.

Dümig A, Häusler W,Steffens M, Kögel-Knabner I. 2012. Clay fractions from a soil chronosequence after glacier retreat reveal the initial evolution of organo–mineral associations. Geochim Cosmochim Acta 85: 1-18.

Esperschütz J, Pérez-de-Mora A, Schreiner K, Welzl G, Buegger F, Zeyer J, Hagedorn F, Munch JC, Schloter M. 2011. Microbial food web dynamics along a soil chronosequence of a glacier forefield. Biogeosciences 8: 3283-3294.

Fierer N, Jackson RB. 2005. The diversity and biogeography of soil bacterial communities. Proc Natl Acad Sci USA 103: 626-631.

Hodkinson ID, Coulson SJ, Webb NR. 2003. Community assembly along proglacial chronosequences in the high Arctic: vegetation and soil development in north-west Svalbard. J Ecol 91: 651-663.

Hugenholtz P, Goebel BM, Pace NR. 1998. Impact of culture-independent studies on the emerging phylogenetic view bacterial diversity. J Bacteriol 180: 4765-4774.

Huggett RJ. 1998. Soil chronosequences, soil development, and soil evolution: a critical review. Catena 32: 155-172.

Hwang K, Oh J, Kim TK, Kim BK, Yu DS, Hou BK, Caetano-Anollés G, Hong SG, Kim KM. 2013. Clustom: a novel

method for clustering 16s rRNA next generation sequences by overlap minimization. PLoS ONE 8: e62623.

IPCC. 2013. Climate change 2013: The physical science basis. Contribution of Working Group I to the Fifth Assessment Report of the Intergovernmental Panel on Climate Change (Stocker TF, Qin D, Plattner G-K, Tignor MMB, Allen SK, Boschung J, Nauels A, Xia Y, Bex V, Midgley PM, eds). Cambridge University Press, Cambridge, and New York, NY, pp. 1–30, doi:10.1017/CBO9781107415324.004.

Jacobson Jr GL, Birks HJB. 1980. Soil development on recent end moraines of the Klutlan Glacier, Yukon Territory, Canada. Quat Res 14: 87-100.

Jangid K, Whitman WB, Condron LM, Turner BL, Williams MA. 2013. Soil bacterial community succession during long-term ecosystem development. Mol Ecol 22: 3415-3424.

Jones RT, Robeson MS, Lauber CL, Hamady M, Knight R, Fierer N. 2009. A comprehensive survey of soil acidobacterial diversity using pyrosequencing and clone library analyses. ISME J 3: 442-453.

Jung JY, Lee K, Lim HS, Kim H, Lee EJ, Lee YK. 2014. Soil organic carbon characteristics relating to geomorphology near Vestre Lovénbreen moraine in Svalard. J Ecol Environ 37: 69-79.

Kim M, Morrison M, Yu Z. 2011a. Evaluation of different partial 16S rRNA gene sequence regions for phylogenetic analysis of microbiomes. J Microbiol Methods 84: 81-87.

Kim OS, Cho YJ, Lee K, Yoon SH, Kim M, Na HS, Park SC, Jeon YS, Lee JH, Yi HN, Won SG, Chun J. 2011b. Introducing EzTaxon-e: a prokaryotic 16S rRNA gene sequence database with phylotypes that represent uncultured species. Int J Syst Evol Microbiol 62: 716-721.

Knelman JE, Legg TM, O'Neill SP, Washenberger CL, González A, Cleveland CC, Nemergut DR. 2012. Bacterial community structure and function change in association with colonizer plants during early primary succession in a glacier forefield. Soil Biol Biochem 46: 172-180.

Kögel-Knabner I, Hatcher PG, Tegelaar EW, Leeuw JW. 1992. Aliphatic components of forest soil organic matter as determined by solid-state ^{13}C NMR and analytical pyrolysis. Sci Total Environ 113: 89-106.

Kume A, Bekku YS, Hanba YT, Kanda H. 2003. Carbon isotope discrimination in diverging growth forms of *Saxifraga oppositifolia* in different successional stages in a High Arctic glacier foreland. Arct Antarct Alp Res 35: 377-383.

Lauber CL, Hamady M, Knight R, Fierer N. 2009. Pyrosequencing-based assessment of soil pH as a predictor of soil bacterial community structure at the continental scale. Appl Environ Microbiol 75: 5111-5120.

Marín-Spiotta E, Swanston CW, Torn MS, Silver WL, Burton SD. 2008. Chemical and mineral control of soil carbon turnover in abandoned tropical pastures. Geoderma 143: 49-62.

Matthews JA. 1992. The ecology of recently-deglaciated terrain: A geoecological approach to glacier forelands and primary succession. Cambridge University, Cambridge.

Messer AC. 1988. Regional variations in rates of pedogenesis and the influence of climatic factors on moraine chronosequences, southern Norway. Arctic Alp Res 20: 31-39.

Miniaci C, Bunge M, Duc L, Edwards I, Bürgmann H, Zeyer J. 2007. Effects of pioneering plants on microbial structures and functions in a glacier forefield. Biol Fertil Soils 44: 289-297.

Moreau M, Laffly D, Joly D, Brossard T. 2005. Analysis of plant colonization on an arctic moraine since the end of the Little Ice Age using remotely sensed data and a Bayesian approach. Remote Sens Environ 99: 244-253.

Moreau M, Mercier D, Laffly D, Roussel E. 2008. Impacts of recent paraglacial dynamics on plant colonization: A case study on Midtre Lovénbreen foreland, Spitsbergen (79°N). Geomorphology 95: 48-60.

Nemergut DR, Anderson SP, Cleveland CC, Martin AP, Miller AE, Seimon A, Schmidt SK. 2007. Microbial community succession in an unvegetated, recently deglaciated soil. Microb Ecol 53: 110-122.

Nilsen L, Brossard T, Joly D. 1999a. Mapping plant communities in a local Arctic landscape applying a scanned infrared aerial photograph in a geographical information system. Int J Remote Sens 20: 463-480.

Nilsen L, Elvebakk A, Brossard T, Joly D. 1999b. Mapping and analysing arctic vegetation: Evaluating a method coupling numerical classification of vegetation data with SPOT satellite data in a probability model. Int J Remote Sens 20: 2947-2977.

Oh J, Kim BK, Cho WS, Hong SG, Kim KM. 2012. PyroTrimmer: a software with GUI for pre-processing 454 amplicon sequences. J Microbiol 50: 766-769.

Paré MC, Bedard-Haughn A. 2011. Optimum liquid density in separation of the physically uncomplexed organic matter in Arctic soils. Can J Soil Sci 91: 65-68.

Philippot L, Tscherko D, Bru D, Kandeler E. 2011. Distribution of high bacterial taxa across the chronosequence of two alpine glacier forelands. Microb Ecol 61: 303-312.

R Development Core Team. 2011. R: A language and environment for statistical computing. R Foundation for Statistical Computing, Vienna.

Reddy GSN, Uttam A, Shivaji S. 2008. *Bacillus cecembensis*

sp. nov., isolated from the Pindari glacier of the Indian Himalayas. Int J Syst Evol Microbiol 58: 2330-2335.

Schloss PD, Westcott SL, Ryabin T, Hall JR, Hartmann M, Hollister EB, Lesniewski RA, Oakley BB, Parks DH, Robinson CJ, Sahl JW, Stres B, Thallinger GG, Van Horn DJ, Weber CF. 2009. Introducing mothur: Open-source, platform-independent, community-supported software for describing and comparing microbial communities. Appl Environ Microbiol 75: 7537-7541.

Schmidt SK, Reed SC, Nemergut DR, Grandy AS, Cleveland CC, Weintraub MN, Hill AW, Costello EK, Meyer AF, Neff JC, Martin AM. 2008. The earliest stages of ecosystem succession in high-elevation (5000 metres above sea level), recently deglaciated soils. Proc R Soc B 275: 2793-2802.

Schulz S, Brankatschk R, Dümig A, Kögel-Knabner I, Schloter M, Zeyer J. 2013. The role of microorganisms at different stages of ecosystem development for soil formation. Biogeosciences 10: 3983-3996.

Schütte UM, Abdo Z, Bent SJ, Williams CJ, Schneider GM, Solheim B, Forney LJ. 2009. Bacterial succession in a glacier foreland of the High arctic. ISME J 3: 1258-1268.

Schütte UM, Abdo Z, Foster J, Ravel J, Bunge J, Solheim B, Forney LJ. 2010. Bacterial diversity in a glacier foreland of the high arctic. Mol Ecol 19: 54-66.

Serreze MC, Walsh JE, Chapin III FS, Osterkamp T, Dyurgerov M, Romanovsky V, Oechel WC, Morison J, Zhang T, Barry RG. 2000. Observational evidence of recent change in the northern high-latitude environment. Clim Change 46: 159-207.

Six J, Conant RT, Paul EA, Paustian K. 2002. Stabilization mechanisms of soil organic matter: Implications for C-saturation of soils. Plant Soil 241: 155-176.

Sohi SP, Mahieu N, Powlson DS, Madari B, Smittenberg RH, Gaunt JL. 2005. Investigating the chemical characteristics of soil organic matter fractions suitable for modeling. Soil Sci Soc Am J 69: 1248-1255.

Thomas GW. 1996. Soil pH and acidity. In: Methods of soil analysis. Part 3. SSSA Book Ser. No. 5 (Sparks DL, ed). Soil Science Society of America Inc., Madison, WI, pp 475-490.

Turicchia S, Ventura S, Schütte U, Soldati E, Zielke M, Solheim B. 2005. Biodiversity of the cyanobacterial community in the foreland of the retreating glacier Midtre Lovènbreen, Spitsbergen, Svalbard. Algol Stud 117: 427-440.

Vishnivetskaya TA, Layton AC, Lau MC, Chauhan A, Cheng KR, Meyers AJ, Murphy JR, Rogers AW, Saarunya GS, Williams DE, Pfiffner SM, Biggerstaff JP, Stackhouse BT, Phelps TJ, Whyte L, Sayler GS, Onstott TC. 2014. Commercial DNA extraction kits impact observed microbial community composition in permafrost samples. FEMS Microbiol Ecol 87: 217-230.

Walker LR, Wardle DA, Bardgett RD, Clarkson BD. 2010. The use of chronosequences in studies of ecological succession and soil development. J Ecol 98: 725-736.

Wallenstein MD, McMahon S, Schime J. 2007. Bacterial and fungal community structure in Arctic tundra tussock and shrub soils. FEMS Microbiol Ecol 59: 428-435.

Wander M. 2004. Soil organic matter fractions and their relevance to soil function. In: Soil organic matter in sustainable agriculture (Magdoff F, Ray RW, eds). CRC Press, Boca Raton, FL, pp 67-102.

White DM, Hodkinson ID, Seelen SJ, Coulson SJ. 2007. Characterization of soil carbon from a Svalbard glacier-retreat chronosequence using pyrolysis–GC/MS analysis. J Anal Appl Pyrol 78: 70-75.

Wu X, Zhang W, Liu G, Yang X, Hu P, Chen T, Zhang G, Li Z. 2012. Bacterial diversity in the foreland of the Tianshan No. 1 glacier, China. Environ Res Lett 7: 014038.

Zumsteg A, Luster J, Göransson H, Smittenberg RH, Brunner I, Bernasconi SM, Zeyer J, Frey B. 2012. Bacterial, archaeal and fungal succession in the forefield of a receding glacier. Microb Ecol 63: 552-564.

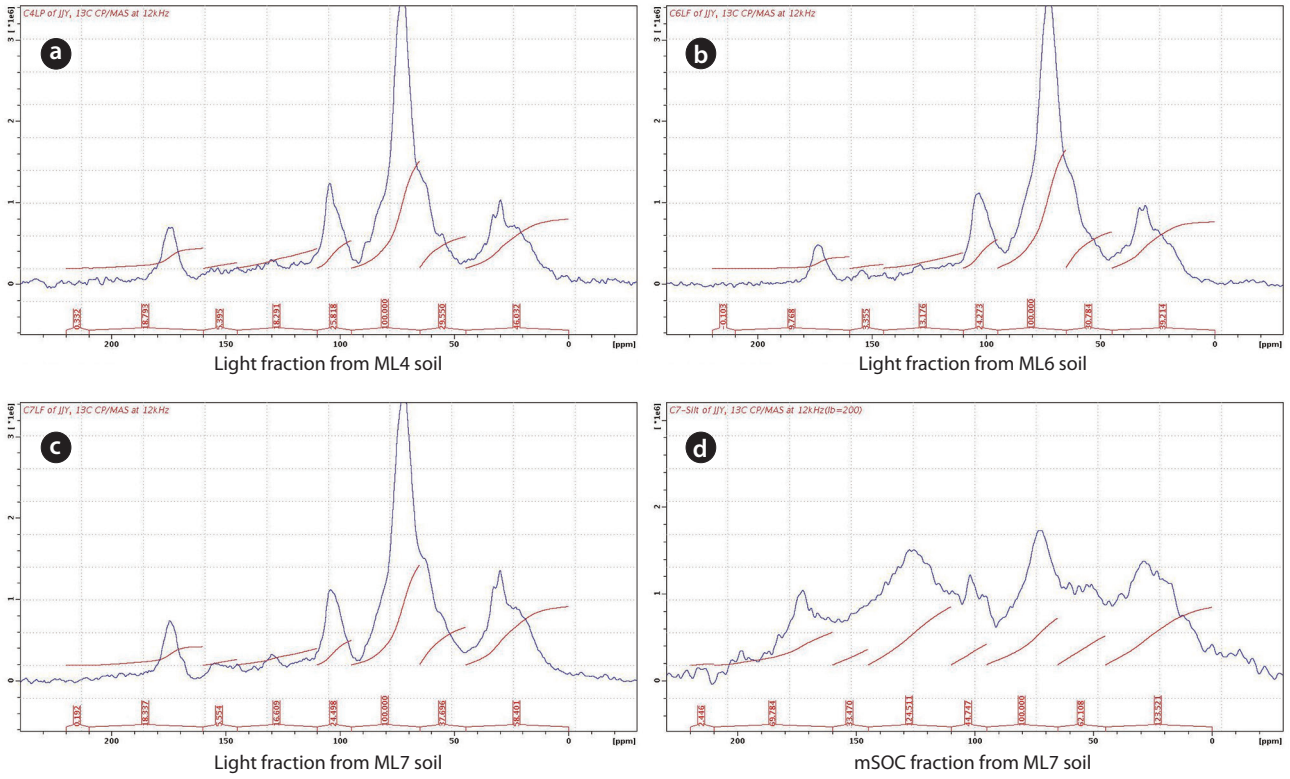

Fig. S1. Solid-state ^{13}C cross polarization/magic angle spinning nuclear magnetic resonance (NMR) spectra from soil organic carbon (SOC) fractions.

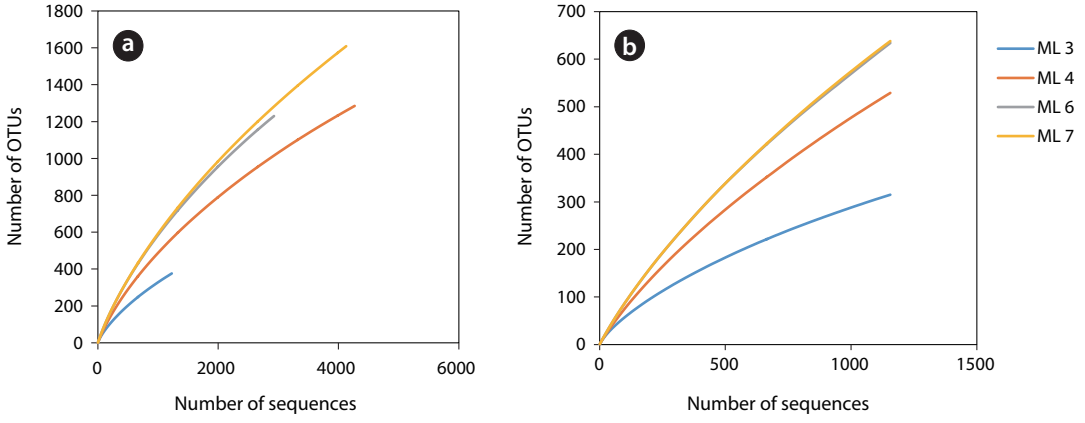

Fig. S2. Comparative analysis of rarefaction curves from original (a) and resampled sequences (b) at the operational transcriptional unit (OTU) level.